

## **Microscopic Theory of Intrinsic Shear and Bulk Viscosities**

**Wokyung Sung,<sup>1,2</sup> John Karkheck,<sup>3</sup> and G. Stell<sup>4</sup>**

*Received May 12, 1981; revised July 28, 1981*

---

A microscopic theory of intrinsic shear and bulk viscosities of solutions is given for a model of particles that interact with hard-sphere cores and weak long-range attraction. The approximation considered (the velocity chaos assumption of the Enskog theory) can be expected to yield quantitatively useful values for viscosities of the model solute-solvent system when the solute particles are not much larger than the solvent particles. Under solute-solvent mixing conditions of constant pressure and temperature we find that the intrinsic viscosities of a hard-sphere solute in a hard-sphere solvent can be positive or negative, depending upon size and mass ratios; for solute and solvent particles whose mass ratio equals their volume ratio, the intrinsic shear and bulk viscosities are always positive for solute particles larger than solvent particles: in the opposite case, the intrinsic shear viscosity is always negative while the intrinsic bulk viscosity is for the most part negative, becoming positive again when the solute particle is sufficiently small. For solute particles smaller than solvent particles, this result is sensitive to change in mass ratio. The addition of solvent-solvent attraction is found to lower the intrinsic viscosities substantially; the addition of solute-solvent attraction raises it. Detailed quantitative analysis of these effects is given.

---

**KEY WORDS:** Kinetic theory; transport coefficients; intrinsic shear viscosity; intrinsic bulk viscosity.

---

<sup>1</sup> Department of Physics, State University of New York at Stony Brook, Long Island, New York 11794.

<sup>2</sup> Present Address: Department of Chemical Engineering, University of Minnesota, Minneapolis, Minnesota 55455.

<sup>3</sup> Department of Mechanical Engineering, State University of New York at Stony Brook, Long Island, New York, 11794.

<sup>4</sup> Departments of Mechanical Engineering and Chemistry, State University of New York at Stony Brook, Long Island, New York 11794.

## 1. INTRODUCTION

In 1906, Einstein derived an expression for the shear viscosity of a dilute suspension of spherical particles in an incompressible fluid.<sup>(1)</sup> The derivation assumes the suspended particles to be large enough compared to the mean free path of fluid particles so that the latter can be regarded as constituting a homogeneous structureless continuum rather than a molecular solvent. The Einstein result can be expressed as

$$\eta = \eta_{10} \left( 1 + \frac{5}{2} \xi_2 \right) \quad (1.1)$$

where  $\eta$  is the shear viscosity of suspension,  $\eta_{10}$  is the pure-fluid viscosity, and  $\xi_2$  the volume fraction of the suspended particles, i.e., the ratio of the total volume of the suspended particles to the total volume of the suspension.

This important result has been generalized to higher particle concentration and to nonspherical shapes.<sup>(2)</sup> To our knowledge, however, very little has been done toward generalizing the Einstein result to the case of a bona-fide molecular solvent of particles into which solute particles of molecular size have been introduced.<sup>5</sup> It is this case that we consider here.

We take as our Hamiltonian model a binary fluid of particles interacting pairwise with hard-sphere repulsion plus weak, long-range attraction. Our results are developed on the basis of the revised Enskog theory (RET) of hard-sphere mixtures<sup>(4)</sup> suitably extended to accommodate the attractive tail of the intermolecular potential. The relevant extension has recently been put on a firm conceptual foundation by Karkheck and Stell.<sup>(5)</sup> The standard Chapman–Enskog procedure<sup>(6)</sup> (in lowest Sonine polynomial approximation) is used to obtain the transport coefficients. In comparing the pure-solvent transport properties to those in the presence of solute, we are mainly interested in our system under the thermodynamic conditions that are usually easiest to handle in the laboratory—fixed temperature and external pressure. The key thermodynamic input needed in our calculation is provided by the equation of state for a binary mixture of hard spheres, which is modified in a simple way by the presence of the attractive tail. We use the equation of state of Mansoori et al.<sup>(7)</sup> (for hard spheres), which is known to be an extremely accurate approximation.

Although by no means exact, the resulting theory can be expected to yield with reasonable accuracy all the trends of the intrinsic shear and bulk

<sup>5</sup> The only previous statistical mechanical study yielding explicit analytic and quantitative results of which we are aware is the interesting exploratory investigation of a hard-sphere system by W. A. McElhannon and E. McLaughlin.<sup>(3)</sup> Their calculations were made without the use of a physically realistic solute–solvent mixing condition, which has important numerical consequences. In addition, we find some calculational mistakes in their work.

viscosities [defined by (2.28) and (2.29)] for monatomic fluids that we wish to study as long as the size of the solute particle is not much larger than its mean free path in solvent. However, we cannot expect the Enskog result to remain meaningful in the hydrodynamic limit, i.e., the limit  $l_{11}/\sigma_{22} \rightarrow 0$ , where  $l_{11}$  is the mean free path of solvent particles and  $\sigma_{22}$  is the diameter of the solute particles. The Enskog theory assumes "velocity chaos," i.e., the lack of dynamic correlation between two particles about to collide, and this assumption prevents an adequate description of certain collective effects involving repeated collisions that appear to be fundamental to the hydrodynamic description. As a result, the Enskog theory yields intrinsic viscosities that become spuriously singular as  $l_{11}/\sigma_{22} \rightarrow 0$ , as we shall see. In this paper we therefore focus mainly on the values of  $l_{11}/\sigma_{22}$  not too much less than unity, for which Enskog theory can be expected to be most useful. We also restrict our attention to values of  $a_{ij}$ , the integrated strength of the attractive potential, that correspond to values for simple mixtures that have been determined from the available thermodynamic data.

The presentation of our work is as follows: In Section 2, we give a brief sketch of our calculation of the intrinsic shear and bulk viscosities from the (revised) Enskog theory of hard spheres. A mixing rule for fixed temperature and pressure is derived. In Section 3 we discuss how the inclusion of an infinitely weak, long-ranged attraction between pairs of molecules perturbs the results of pure hard-core repulsion. This is found to yield a nonnegligible contribution to the intrinsic quantities under our thermodynamic mixing condition. In Section 4 we give quantitative results and a discussion.

## 2. ENSKOG THEORY OF THE INTRINSIC SHEAR AND BULK VISCOSITIES FOR A HARD-SPHERE FLUID

Our starting point is the revised Enskog equation<sup>(4)</sup> that reads

$$\left( \frac{\partial}{\partial t} + \mathbf{V}_i \cdot \nabla \right) f_i(\mathbf{r}, \mathbf{V}_i, t) = \sum_j J_{ij} \quad (i, j = 1, 2) \quad (2.1)$$

with the collision integral

$$\begin{aligned} J_{ij} = & \sigma_{ij}^2 \int d\mathbf{V}_j d\boldsymbol{\sigma} (\boldsymbol{\sigma} \cdot \mathbf{V}_{ji}) \Theta(\boldsymbol{\sigma} \cdot \mathbf{V}_{ji}) \\ & \times \left[ g_{ij}(\mathbf{r}, \mathbf{r} + \sigma_{ij}\boldsymbol{\sigma}) f_i(\mathbf{r}, \mathbf{V}'_i, t) f_j(\mathbf{r} + \sigma_{ij}\boldsymbol{\sigma}, \mathbf{V}'_j, t) \right. \\ & \left. - g_{ij}(\mathbf{r}, \mathbf{r} - \sigma_{ij}\boldsymbol{\sigma}) f_i(\mathbf{r}, \mathbf{V}_i, t) f_j(\mathbf{r} - \sigma_{ij}\boldsymbol{\sigma}, \mathbf{V}_j, t) \right] \quad (2.2) \end{aligned}$$

where  $f_i$  is one particle distribution function (DF) of the species  $i$ ,  $\sigma_{ij}$  is the contact distance between the center of the particle  $i$  and  $j$ ,  $\mathbf{V}_{ji} = \mathbf{V}_j - \mathbf{V}_i$ ,

the primes in the velocity denote the postcollisional values,  $\sigma$  is the unit vector along the apse line in such a direction that the Heaviside step function  $\Theta(\sigma \cdot \mathbf{V}_{ji})$  imposes the condition of the collision.  $g_{ij}$  is the contact value of the local equilibrium pair distribution function of a nonuniform system, which depends functionally on the local density fields. This dependence represents the difference that distinguishes the revised Enskog theory (RET) from the standard (original) Enskog theory (SET) which replaces  $g_{12}$  by  $Y_{ij}$ , the contact value of the equilibrium pair DF for a *uniform* system, evaluated as a function of the density midway between the centers of the two particles.<sup>(8)</sup> The RET overcomes a number of inadequacies and difficulties of the SET, especially when applied to a mixture.<sup>(9,10)</sup> With regard to our final result for the shear and bulk viscosities, however, we shall see no difference between the two theories.

The hydrodynamic equation for change of mass, momentum, and energy can be constructed from (2.2) by multiplying by  $m_i$ ,  $m_i \mathbf{V}_i$ , and  $\frac{1}{2} m_i \mathbf{V}_i^2$ , respectively, integrating with respect to  $\mathbf{V}_i$  and summing over  $i = 1, 2$ . Since our interest here lies in the viscosities, only the equation for the change of momentum is considered:

$$\rho \left( \frac{\partial \mathbf{u}}{\partial t} + \mathbf{u} \cdot \nabla \mathbf{u} \right) = -\nabla \cdot \mathbf{P} \quad (2.3)$$

where the hydrodynamic variables  $\rho$ ,  $\mathbf{u}$ ,  $\mathbf{P}$  (mass density, velocity, pressure tensor, respectively) are defined through the relations

$$\rho = \sum_{i=1,2} \int f_i m_i d\mathbf{V}_i \quad (2.4)$$

$$\rho \mathbf{u} = \sum_{i=1,2} \int f_i m_i \mathbf{V}_i d\mathbf{V}_i \quad (2.5)$$

$$\mathbf{P} = \mathbf{P}_K + \mathbf{P}_C$$

$$\mathbf{P}_K = \sum_{i=1,2} \int f_i m_i (\mathbf{V}_i - \mathbf{u})(\mathbf{V}_i - \mathbf{u}) d\mathbf{V}_i \quad (2.6)$$

$$\begin{aligned} \mathbf{P}_C = & \sum_{i,j=1,2} \frac{1}{2} \sigma_{ij}^3 \int d\mathbf{V}_j d\mathbf{V}_i d\sigma \Theta(\sigma \cdot \mathbf{V}_{ji}) (\sigma \cdot \mathbf{V}_{ji}) \sigma (m_i \mathbf{V}_i' - m_i \mathbf{V}_i) \\ & \times \int_0^1 d\alpha g_{ij}(\mathbf{r} - \alpha \sigma_j \sigma, \mathbf{r} - \alpha \sigma_j \sigma + \sigma_j \sigma) \\ & \times f_i(\mathbf{r} - \alpha \sigma_j \sigma, \mathbf{V}_i, t) f_j(\mathbf{r} - \alpha \sigma_j \sigma + \sigma_j \sigma, \mathbf{V}_j, t) \end{aligned} \quad (2.7)$$

In (2.7)  $\mathbf{P}_C^{(11)}$  is identified as the collisional momentum transfer not included in the Boltzman-equation description. To evaluate  $\mathbf{P}$ , one should solve for  $f_i$ . The Chapman-Enskog procedure of normal solution for  $f_i$  is

known to provide an adequate means of yielding the hydrodynamic transport coefficients. We shall not elaborate here this standard procedure in detail but present the final results. For  $\mathbf{P}$ , we find up through linear order in gradient in the hydrodynamic velocity  $\mathbf{u}$

$$\mathbf{P} = P\mathbf{I} - \eta[\nabla\mathbf{u} + (\nabla\mathbf{u})^T - \frac{2}{3}\nabla \cdot \mathbf{u}\mathbf{I}] - \kappa\nabla \cdot \mathbf{u} \quad (2.8)$$

Thus, with this constitutive relation, (2.3) becomes the Navier–Stokes equation with  $\eta$ ,  $\kappa$  the shear and bulk viscosities, now given microscopically. The  $\eta$ ,  $\kappa$  are given by

$$\eta = \eta_1 + \eta_2 + \eta_3 \quad (2.9)$$

$$\eta_1 = \frac{1}{2}kT \sum_{i=1,2} n_i b_0^{(i)}$$

$$\eta_2 = \frac{4\pi kT}{15} \sum_{i,j=1,2} \frac{\mu_{ij}}{m_i} \beta_{ij}^{(3)} b_0^{(i)}$$

$$\eta_3 = \frac{4}{15} \sum_{i,j=1,2} P_{ij} \beta_{ij}^{(4)}$$

$$\kappa = \kappa_1 + \kappa_2 \quad (2.10)$$

$$\kappa_1 = \frac{4\pi kT}{3} \sum_{i,j=1,2} \frac{\mu_{ij}}{m_i} \beta_{ij}^{(3)} h_1^{(i)}$$

$$\kappa_2 = \frac{4}{9} \sum_{i,j=1,2} \beta_{ij}^{(4)} p_{ij}$$

Here  $b_0^{(i)}$ ,  $h_1^{(i)}$ , the coefficients of the lowest-order Sonine polynomial<sup>(6)</sup> that is used in our approximation, are to be obtained from the conditions<sup>(8,12)</sup>

$$\begin{aligned} &8 \sum_{j=1,2} \beta_{ij}^{(2)} p_{ij} \frac{\mu_{ij}}{m_i} \left( \frac{b_0^{(i)}}{m_i} + \frac{b_0^{(j)}}{m_j} - \frac{5}{3} \frac{b_0^{(j)} - b_0^{(i)}}{m_j} \right) \\ &= 5n_i + \frac{8\pi}{3} \sum_{j=1,2} \beta_{ij}^{(3)} \frac{\mu_{ij}}{m_i} \end{aligned} \quad (2.11)$$

$$\sum_{i=1,2} n_i h_1^{(i)} = 0 \quad (2.12a)$$

$$8 \sum_{j=1,2} \beta_{ij}^{(2)} p_{ij} (h_1^{(j)} - h_1^{(i)}) M_{ij}^{-1} = -n_i + \frac{n_i P}{nkT} - \frac{4\pi}{3} \sum_{j=1,2} \beta_{ij}^{(3)} \frac{m_j}{M_{ij}} \quad (2.12b)$$

(In Ref. 13 we show that the lowest-order Sonine approximation is accurate in this application except for the case  $m_2/m_1 \rightarrow 0$ .) The  $Y_{ij}$  is the contact value of the equilibrium pair distribution function,  $n_i$  is the number density of the species  $i$ ,  $n = n_1 + n_2$ ,  $\mu_{ij} = m_i m_j / m_i + m_j$ ,  $M_{ij} = m_i + m_j$ ,  $\sigma_{ij}$

$= \frac{1}{2}(\sigma_{ii} + \sigma_{jj})$ ,  $\beta_{ij}^{(l)} = \sigma_{ij}^l n_i n_j Y_{ij}$ ,  $p_{ij} = (2\pi k T \mu_{ij})^{1/2}$ . For the pressure, we have

$$P = kT \left( n + \frac{2\pi}{3} \sum_{i,j=1,2} \beta_{ij}^{(3)} \right) \quad (2.13)$$

The calculations for the explicit  $\eta$  and  $\kappa$  are very tedious but straightforward. Since we shall concern ourselves with the intrinsic viscosities [defined by (2.28) and (2.29)], we expand  $\eta$ ,  $\kappa$  up to the linear order in the solute volume fraction  $\xi_2$ , keeping the ratio of the other parameters arbitrary:

$$\eta = (\eta)_0 + \xi_2 (\eta)_1 \quad (2.14)$$

$$\begin{aligned} (\eta)_0 &= \left[ \frac{1}{Y_{11}^0} \left( 1 + \frac{8}{5} \xi_1 Y_{11}^0 \right)^2 + \frac{768}{25\pi} \xi_1^2 Y_{11}^0 \right] \eta_1^B \\ (\eta)_1 &= \left\{ \frac{1}{Y_{11}^0} \left( 1 + \frac{8}{5} \xi_1 Y_{11}^0 \right) \left[ \frac{2}{5} (1+q)^3 \left( 1 + \frac{\mu_{12}}{m_1} \right) Y_{12}^0 - \frac{Y_{11,2}^0}{Y_{11}^0} + \frac{8}{5} \xi_1 Y_{11,2}^0 \right] \right. \\ &\quad + \left[ \frac{768}{25\pi} \xi_1^2 Y_{11,2}^0 + \frac{96}{25\pi} \left( \frac{2\mu_{12}}{m_1} \right)^{1/2} (1+q)^4 q^{-1} \xi Y_{12}^0 \right] \\ &\quad + \xi_1^{-1} \left( 1 + \frac{2}{3} \frac{\mu_{12}}{m_1} \right)^{-1} \frac{1}{Y_{11}^0} \left( 1 + \frac{8}{5} \xi_1 Y_{11}^0 \right) \\ &\quad \times \left[ \frac{2}{3} q^3 \frac{\mu_{12}}{m_1} - \frac{5}{12} q (1+q)^2 \left( \frac{2\mu_{12}}{m_1} \right)^{1/2} \right. \\ &\quad \times \left. \frac{1}{Y_{11}^0} \left( 1 + \frac{8}{5} \xi_1 Y_{11}^0 \right) Y_{12}^0 + \frac{2}{5} \left( \frac{\mu_{12}}{m_1} - 1 \right) (1+q)^3 \xi_1 Y_{12}^0 \right] \\ &\quad + \xi_1^{-1} \left( 1 + \frac{2}{3} \frac{\mu_{12}}{m_1} \right)^{-1} \\ &\quad \times \left[ \frac{2}{3} \left( \frac{\mu_{12}}{m_1} \right) \frac{1}{Y_{11}^0} \left( 1 + \frac{8}{5} \xi_1 Y_{11}^0 \right) + 4 \left( (1+q)^2 \left( \frac{2\mu_{12}}{m_1} \right)^{1/2} pq \right)^{-1} \right. \\ &\quad \times \left. Y_{12}^0 \left( q^3 + \frac{2}{5} (1+q)^3 p \frac{\mu_{12}}{m_1} \xi_1 Y_{12}^0 \right) \right] \\ &\quad \left. \times \left( q^3 + \frac{2}{5} (1+q)^3 p \frac{\mu_{12}}{m_1} \xi_1 Y_{12}^0 \right) \right\} \eta_1^B \end{aligned}$$

$$\begin{aligned} \kappa &= (\kappa)_0 + \xi_2(\kappa)_1 & (2.15) \\ (\kappa)_0 &= \frac{256}{5\pi} \xi_1^2 Y_{11}^0 \eta_1^B \\ (\kappa)_1 &= \left\{ \frac{256}{5\pi} \xi_1^2 Y_{11,2}^0 + \frac{32}{5\pi} \left( \frac{2\mu_{12}}{m_1} \right)^{1/2} q^{-1} (1+q)^4 \xi_1 Y_{12}^0 \right. \\ &\quad \left. + \frac{64\sqrt{2}}{5} \left( \frac{\mu_{12}}{m_1} \right)^{-3/2} [pq(1+q)^2]^{-1} \right. \\ &\quad \left. \times Y_{12}^0 \left[ q^3 \frac{Y_{11}^0}{Y_{12}^0} - \frac{1}{4} (1+q)^3 p \frac{\mu_{12}}{m_1} \right]^2 \right\} \eta_1^B \end{aligned}$$

Here

$$\begin{aligned} p &= m_1/m_2, & q &= \sigma_{11}/\sigma_{22}, & \xi_i &= \frac{\pi}{6} n_i \sigma_{ii}^3, & \eta_1^B &= \frac{5}{16} \left( \frac{m_1 kT}{\pi} \right)^{1/2} \frac{1}{\sigma_{11}^2} \\ Y_{ij}^0 &= Y_{ij}|_{\xi_2=0}, & Y_{ij,k}^0 &= \frac{\partial}{\partial \xi_k} Y_{ij} \Big|_{\xi_2=0} \end{aligned}$$

For the pressure, we find

$$\begin{aligned} P &= (P)_0 + \xi_2(P)_1 \\ (P)_0 &= n_1 kT (1 + 4\xi_1 Y_{11}^0) & (2.16) \\ (P)_1 &= n_1 kT [4\xi_1 Y_{11,2}^0 + (1+q)^3 Y_{12}^0] \end{aligned}$$

The viscosities and pressure in the pure solvent are obtained by substituting  $\xi_1^0, n_1^0$  (pure solvent volume-fraction and number density) for  $\xi_1, n_1$  in  $(\eta)_0, (\kappa)_0$ , and  $(P)_0$ :

$$\eta_{10} = \left\{ \frac{1}{Y_{11}^0(\xi_1^0)} \left[ 1 + \frac{8}{5} \xi_1^0 Y_{11}^0(\xi_1^0) \right]^2 + \frac{768}{25\pi} \xi_1^{0^2} Y_{11}^0(\xi_1^0) \right\} \eta_1^B \quad (2.17)$$

$$\kappa_{10} = \left[ \frac{256}{5\pi} \xi_1^{0^2} Y_{11}^0(\xi_1^0) \right] \eta_1^B \quad (2.18)$$

$$P_{10} = n_1^0 kT [1 + 4\xi_1^0 Y_{11}^0(\xi_1^0)] \quad (2.19)$$

In order to compare the viscosities of the suspension with those of the pure solvent, the thermodynamic conditions of both systems should be specified. We shall assume, in mixing, fixed conditions of temperature, total solvent mass, and external pressure, which represents the most common experimental situation. To show how this condition differentiates  $\xi_1$  from

$\xi_1^0$ ,  $Z = P/kT$  is expanded up through the deviation linear in  $\xi_2$ :

$$Z = Z_0 + \left( \frac{\partial Z}{\partial \xi_1} \right)_0 (\xi_1 - \xi_1^0) + \left( \frac{\partial Z}{\partial \xi_2} \right)_0 \xi_2 \quad (2.20)$$

where 0 refers to the pure solvent, i.e., the point ( $\xi_1 = \xi_1^0, \xi_2 = 0$ ). By substituting the mixing rule in the form

$$\xi_1 = \xi_1^0(1 - M\xi_2) \quad (2.21)$$

and by noting that  $Z = Z_0$ , we find

$$\begin{aligned} M &= \left( \frac{\partial Z}{\partial \xi_2} \right)_0 / \xi_1^0 \left( \frac{\partial Z}{\partial \xi_1} \right)_0 \\ &= \left( \frac{\partial P}{\partial \xi_2} \right)_0 / \xi_1^0 \left( \frac{\partial P_{10}}{\partial \xi_1^0} \right) \end{aligned} \quad (2.22)$$

Substituting (2.16), (2.19), we find for the hard spheres

$$M_H = \frac{1}{\xi_1^0} \frac{q^3 + (1+q)^3 \xi_1^0 Y_{12}^0 + 4\xi_1^{0^2} Y_{11,2}^0}{1 + 8\xi_1^0 Y_{11}^0 + 4\xi_1^{0^2} Y_{11,1}^0} \quad (2.23)$$

This also can be expressed as

$$M = \beta_1^0 \left( \frac{\partial P}{\partial \xi_2} \right)_0 \quad (2.24)$$

where  $\beta_1^0$  is the isothermal compressibility of pure solvent defined as

$$\beta_1^0 = - \frac{1}{V_0} \left( \frac{\partial V_0}{\partial P_{10}} \right)_T = \left( n_1^0 \frac{\partial P_{10}}{\partial n_1^0} \right)_T^{-1} \quad (2.25)$$

For the fluid of general intermolecular interaction, (2.22) and (2.24) will provide a means of determining  $M$  through thermodynamic measurements.

The simplest and most illuminating expression for  $M$  in the operational sense is simply given as follows: Consider a sample volume  $V_0$  of the pure solvent. By adding an infinitesimally small amount of the solute particles, the overall volume also will generally increase infinitesimally ( $\Delta V$ ). The volume fraction of the solvent particles would be affected according to the relation

$$\xi_1 = \frac{N_1 v_1}{V_0 + \Delta V} = \xi_1^0 \left( 1 - \frac{\Delta V}{V_0} \right) \quad (2.26)$$

where  $v_1, N_1$  are the molecular volume and the total number of the solvent particles. By comparing this with (2.21), we find

$$M = \Delta V / V_2 \quad (2.27)$$



where  $V_2 = N_2 v_2$  is the total volume of the solute mixed. Thus, determination of  $M$  requires only a simple experiment of measuring the volume overflow  $\Delta V$ .

Let us imagine the case in which the solute particles are macroscopically large. Our macroscopic experience immediately tells us that  $M_H = 1$  in this limit, since in hard-sphere repulsion there is no solvation effect, i.e.,  $V_2 = \Delta V$ . In fact, when the Mansoori-Carnahan-Starling-Leland (MCSL)<sup>(7)</sup> approximation for  $Y_{ij}$  (see Appendix) is used, (2.23) gives in this limit a value ranging from 0.98 to 1 for any  $\xi_1^0$ . This remarkably slight deviation from unity suggests strongly the possibility that the MCSL remains a good approximation in the  $q \rightarrow 0$  limit for all solvent density.

With the mixing rule (2.21), (2.23), we are now in a position to evaluate the intrinsic viscosities defined by<sup>6</sup>

$$\{\eta\} \equiv \lim_{\xi_2 \rightarrow 0} \frac{\eta - \eta_{10}}{\xi_2 \eta_{10}} \tag{2.28}$$

$$\{\kappa\} \equiv \lim_{\xi_2 \rightarrow 0} \frac{\kappa - \kappa_{10}}{\xi_2 \eta_{10}} \tag{2.29}$$

We find from (2.14) and (2.15)

$$\{\eta\} = -M_H \xi_1^0 \frac{1}{\eta_{10}} \frac{\partial(\eta)_0}{\partial \xi_1^0} + \frac{(\eta)_1}{\eta_{10}} \Bigg|_{\xi_1 = \xi_1^0} \tag{2.30}$$

$$\{\kappa\} = -M_H \xi_1^0 \frac{1}{\eta_{10}} \frac{\partial \kappa_{10}}{\partial \xi_1^0} + \frac{(\kappa)_2}{\eta_{10}} \Bigg|_{\xi_1 = \xi_1^0} \tag{2.31}$$

Figures 1 and 2 show trends in  $\{\eta\}$  and  $\{\kappa\}$  for the case  $p^{-1} \equiv m_2/m_1 = (\sigma_{22}/\sigma_{11})^\alpha$  ( $\alpha = 0, 2, 3, 4$ ) for  $\xi_1^0 = 0.4$ , the volume fraction of the typical dense liquid. A remarkable feature, first of all, is the divergence that goes as  $q^{-1} = \sigma_{22}/\sigma_{11}$  in the limit  $q \rightarrow 0$ . Since the term responsible for this divergence in (2.14) and (2.15) is precisely proportional to  $\sigma_{22}/l_{11} = 6\sqrt{2} \xi_1 Y_{11} q^{-1}$ , where  $l_{11} = 1/(\sqrt{2} \pi n_1 \sigma_{11}^2 Y_{11})$  is the mean free path of solvent-solvent collision, we naturally expect the hydrodynamic description

<sup>6</sup> Our definition of the intrinsic shear viscosity is nondimensional and thus different from the conventional one which carries the dimension of inverse mass density:

$$[\eta] = \lim_{c_2 \rightarrow 0} \frac{\eta - \eta_{10}}{c_2 \eta_{10}}$$

where  $c_2 = n_2 m_2$ . We also define the intrinsic bulk viscosity in terms of  $\eta_{10}$  rather than  $\kappa_{10}$ , since  $\kappa_{10}$  vanishes in the low-density limit.

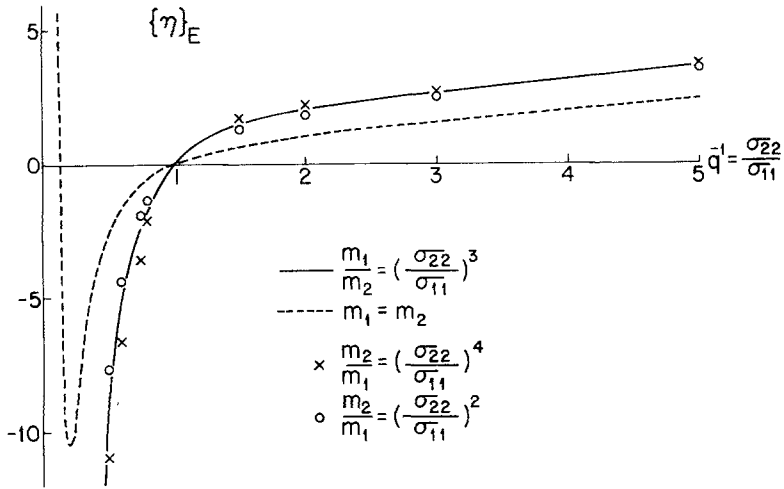


Fig. 1. Intrinsic shear viscosity vs.  $\sigma_{22}/\sigma_{11}$  at solvent volume fraction  $\xi_1^0 = 0.4$ . The case  $m_2/m_1 = (\sigma_{22}/\sigma_{11})^3$  is denoted by a solid line, the case  $m_1 = m_2$  by a dashed line, the case  $m_2/m_1 = (\sigma_{22}/\sigma_{11})^2$  by open circles, and the case  $m_2/m_1 = (\sigma_{22}/\sigma_{11})^4$  by crosses.

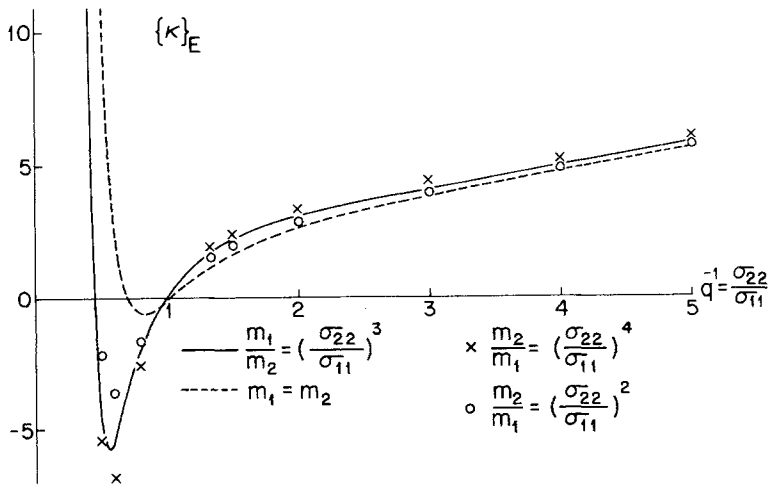


Fig. 2. Intrinsic bulk viscosity vs.  $\sigma_{22}/\sigma_{11}$  at solvent volume fraction  $\xi_1^0 = 0.4$ . Conditions and notations as in Fig. 1.

(in which the solvent is regarded as a structureless continuum on the length scale of the size of solute particle) to yield the exact result in this limit. Since the intermolecular force between the solute and solvent particles is a hard-sphere repulsion which lacks a tangential component, the macroscopic collective manifestation of the solute-solvent interaction results in the form of slip boundary condition for the hydrodynamic variables on the surface of the solute particle. Hydrodynamic calculation with this boundary condition yields  $\{\eta\} = 1$ ,  $\{\kappa\} = 4/3 + \kappa_{10}/\eta_{10}$ .<sup>(13)</sup> (The famous Einstein formula  $\{\eta\} = 5/2$  will only result from an anisotropic molecular interaction that allows transfer of angular momentum at collision, permitting the usual stick boundary condition.)

The reason for this pathological divergence in our kinetic theory calculation is due to the velocity chaos assumption that breaks down badly in this limit, in which the solvent particles near to the large solute particle are likely to make repeated (correlated) collisions with it.<sup>(14)</sup> The resulting singularity of  $O(\sigma_{22}/l_{11})$  in  $\{\eta\}$ ,  $\{\kappa\}$  is similar to that which appears in the Enskog binary diffusivity, in comparison with the hydrodynamic (Stokes-Einstein) result.

However, for  $\sigma_{22}/l_{11}$  small such that a specific pair of solute and solvent particles does not recollide frequently one might expect the velocity-chaos assumption for the solute-solvent collision to better retain its validity. This tendency has been observed in the case of binary diffusion through molecular dynamics studies even at solvent density as high as  $\xi_1 = 0.5$ .<sup>(15)</sup> This tendency and the fact that the Enskog results satisfy the exact symmetry conditions that force  $\{\eta\}$  and  $\{\kappa\}$  to vanish at  $q = 1 = p$  strongly suggest that Figs. 1 and 2 represent the trends of  $\{\eta\}$ ,  $\{\kappa\}$  for hard spheres with reasonable accuracy in the region  $q^{-1} \lesssim 1$ , i.e., the region where the aforementioned singularity ( $q^{-1}$ ) is not appreciable. In addition to the Enskog approximation embedded in Eqs. (2.14), (2.15), and Figs. 1 and 2 one has the approximations introduced in getting the transport coefficients from the Enskog equation. Since the Chapman-Enskog normal solution that we use is appropriate in our study of transport coefficients of the mixture regarded as homogeneous continuum, the only approximation involved is from the use of the lowest Sonine polynomial. In a forthcoming paper,<sup>(13)</sup> we will show this approximation is reasonably accurate as long as the mass of the solute particle is not too small.

In the intermediate region of  $q$ ,  $\{\eta\}$  and  $\{\kappa\}$  must vanish at the point  $q = 1 = p$ , which is no more than a statement of identity of two species. Inclusion of molecules identical to those of the solvent under constant pressure and temperature does not affect the property of the initial system.

Finally we note from Figs. 1 and 2 that our way of classifying the mixture via  $p = q^\alpha$ , albeit somewhat artificial, shows how the intrinsic

viscosities are sensitive to the mass ratio. As one might expect, the result is more insensitive to the mass ratio (i.e., the solute-solvent collisional detail) for the larger solute particle; we find for all values  $\alpha$  in the domain  $1 < \alpha < 5$  the results approach a single asymptote in the limit  $q \rightarrow 0$ . In the opposite limit, however, the result is very sensitive to the mass ratio.

Consider the situation in which both the solvent and solute are so dilute that the mean free path  $l_{ij}$  (of collision between the particles of species  $i$  and  $j$ ) is much larger for all  $i$  and  $j$  than the size of the solute and solvent particles. In that regime, the velocity correlation as well as the spatial correlation is absent ( $g_{ij} = 1$ ); therefore the Boltzmann equation description should correctly apply. It should be noted, however, that we would not have arrived at the low-density expression of  $\{\eta\}$ , had we started with the Boltzmann equation in deriving the intrinsic quantities. Since in the Boltzmann-equation description  $Y_{ij} = 1$  and shear viscosity for the single component is the density-independent  $\eta_1^B$ , our result in the low-density limit would differ in the additional terms [i.e.,  $-M_H \xi_1^0 / \eta_{10} \partial(\eta)_0 / \partial \xi_1^0$ ] and in the part involving  $Y_{11,2}$  in  $(\eta)_1$  (which are generally nonvanishing altogether) from the Boltzmann-equation result given in Chapman and Cowling.<sup>(6)</sup> For the bulk viscosity, which the Boltzmann equation is incapable of yielding, we find a very interesting fact: Although the pure solvent of low density does not have bulk viscosity, it does have the intrinsic bulk viscosity given by  $(\kappa)_1$ , that is,

$$\{\kappa\} = \frac{4\sqrt{2}}{5} \left( \frac{\mu_{12}}{m_1} \right)^{-3/2} [pq(1+q)^2]^{-1} \left[ q^3 - \frac{1}{4}(1+q)^3 p \frac{\mu_{12}}{m_1} \right]^2 \quad (2.32)$$

(The Boltzmann-equation results for intrinsic viscosities are wrong here because the intrinsic viscosities involve *derivatives* with respect to concentration—e.g., intrinsic shear viscosity involves  $\partial(\eta)_0 / \partial \xi_1^0$  as well as the concentration dependence of  $Y_{11,2}$ . These quantities involve an order of concentration dependence—that of the second virial coefficient—that is entirely neglected in the Boltzmann equation, which yields an ideal-gas level of description in this regard.)

### 3. INCLUSION OF THE INFINITELY WEAK AND LONG-RANGED ATTRACTION

It is well known that the hard-sphere model, though crude, represents the main features of the dense fluid structure and is successful in correlating the data of the transport coefficients of real dense fluids in various ways.<sup>(16)</sup> These facts lend support to the view that a workable perturbation theory of the transport can be developed with hard-sphere fluid taken as a reference system. This scheme has already produced fruitful results in regard to thermodynamic properties.

We shall consider here the perturbation in the form of the weak and long-ranged attraction (van der Waal's attraction) added to the hard-core repulsion. The intermolecular potential is written as

$$\phi(r) = \phi_H + \gamma^3 \phi_L(\gamma r) \tag{3.1}$$

where the smallness parameter  $\gamma$  is the inverse of the range of the attractive force.

Resibois et al.<sup>(17)</sup> discovered that the leading effect of the perturbation on the shear and bulk viscosities is in the order of  $\gamma$ :

$$X(\gamma) = X_H + O(\gamma) \tag{3.2}$$

Thus, the transport coefficients are those of the hard-sphere reference system in the limit  $\gamma \rightarrow 0$ . However, as is well known, the thermodynamic properties are different in a significant way<sup>(18)</sup>: For the free energy and pressure we have

$$A = A_H + an^2/kT \tag{3.3}$$

$$p = p_H - an^2 \tag{3.4}$$

where

$$\begin{aligned} -2a &= \lim_{\gamma \rightarrow 0} \gamma^3 \int_{\sigma_{11}}^{\infty} \phi_L(\gamma r) d\mathbf{r} \\ &= \int_0^{\infty} \phi_L(x) dx \end{aligned} \tag{3.5}$$

but for the radial distribution function at its contact value, we get

$$Y_{ij}(\sigma_{ij}) = Y_{ij}^H(\sigma_{ij}) + O(\gamma^3) \tag{3.6}$$

With the hard-sphere pressure  $P_H$  given by the Percus–Yevick compressibility expression or by the more exact form of Carnahan and Starling<sup>(19)</sup> (see Appendix), (3.4) is a modified van der Waals equation of state which yields reasonable thermodynamics for the monatomic fluids.<sup>(20)</sup>

The generalization of (3.5) to binary mixtures is achieved by the van der Waals prescription<sup>(21)</sup>

$$n^2 a = \sum_{i,j=1,2} n_i n_j a_{ij} \tag{3.7}$$

where

$$\begin{aligned} -2a_{ij} &= \lim_{\gamma \rightarrow 0} \gamma^3 \int_{\sigma_{ij}}^{\infty} \phi_L^{ij}(\gamma r) d\mathbf{r} \\ &= \int_0^{\infty} \phi_L^{ij}(x) dx \end{aligned} \tag{3.8}$$

and by (2.13)

$$\frac{P_H}{kT} = n + \frac{2\pi}{3} \sum_{i,j} n_i n_j \sigma_{ij}^3 Y_{ij}$$

In our calculation of the excess transport properties, the inclusion of the perturbation is expected to give a significant contribution, via our thermodynamic mixing function  $M$  (2.21). From (2.22), (2.16), (2.19) we find

$$\begin{aligned} M &= M_H + \Delta M \\ &= \frac{1}{\xi_1^0} \frac{q^3 + (1+q)^3 \xi_1^0 (Y_{12}^0 - b_{12}) + 4\xi_1^{0^2} Y_{11,2}^0}{1 + 8\xi_1^0 (Y_{11}^0 - b_{11}) + 4\xi_1^{0^2} Y_{11,1}^0} \end{aligned} \quad (3.9)$$

where  $b_{ij} = (3/2\pi)a_{ij}\sigma_{ij}^{-3}/kT$ . The intrinsic viscosities are obtained by replacing  $M_H$  by this  $M$  in the expression (2.30), (2.31). In the case that two components are identical, i.e.,  $q = 1$ ,  $b_{11} = b_{12} = b_{22}$ , we find

$$M = M_H = 1/\xi_1^0 \quad (3.10)$$

However, if the two species are identical in mass and size but internally dissimilar in such a way that  $a_{11} \neq a_{12}$ ,  $\Delta M$  does not vanish. Specifically when  $a_{11} > a_{12}$ , we have  $\Delta M > 0$ , and the mixing results in a decrease of the viscosities by

$$-\Delta M \xi_1^0 \frac{1}{X_{10}} \frac{\partial X_{10}}{\partial \xi_1^0}$$

In the opposite case, the opposite result will be found. These intuitively obvious results stem from the fact that the increase of attraction by mixing ( $a_{11} < a_{12}$ ) leads to greater compression than that given by (3.10).

### Determination of $a_{ij}$

The expressions (3.3)–(3.8) do not yield a unique means of finding  $a_{ij}$  and  $\sigma_{ij}$  that are appropriate to the study of real fluids, since real fluids do not have thermodynamics precisely given by these equations. Procedures to find  $a_{ij}$  and  $\sigma_{ij}$  that yield reasonable approximations to the true thermodynamics are well known, however. We shall use the values of  $a_{ij}$  and  $\sigma_{ij}$  that were determined by Snider and Herrington<sup>(22)</sup> from thermodynamic data for simple binary mixtures composed of the almost spherical molecules. They made their determination first for pure fluids by comparing thermodynamic data (PVT) and the latent heat of vaporization, with the equation (3.4) and the expressions for the molar entropy or enthalpy of vaporization that they obtained. In order to obtain  $a_{12}$ , they matched their expressions for the excess Gibbs free energy with the measured data. With these semiempirical values of  $a_{ij}$ ,  $\sigma_{ij}$ , they predicted the excess enthalpy and entropy of mixtures with successful agreement with the measured data.

Snider and Herrington used the Percus–Yevick hard-sphere equation of state to evaluate the hard sphere term  $P_H$  in (3.4), rather than the slightly

more accurate MCSL result<sup>(7)</sup> used by us, but this can be expected to make a negligible difference in the values of  $a_{ij}$  and  $\sigma_{ij}$ . Such fine points are inconsequential to our goal of determining the general trends that will result from the inclusion of attractive potentials that are of the same order of integrated strength as those found in typical fluid mixtures.

#### 4. RESULTS AND DISCUSSION

Summing up the contributions from the Enskog result for hard spheres and from the weak and long-range attraction, we have

$$\begin{aligned} \{X\} &= \{X_E\} + \Delta\{X\}_a \\ &= -\frac{1}{X_{10}} \left( \frac{\partial X_{10}}{\partial \xi_1^0} \right) M \xi_1^0 + \frac{(X)_1}{X_{10}} \Big|_{\xi=\xi^0} \end{aligned} \tag{4.1}$$

where  $X$  is either  $\eta$  or  $\kappa$ .

In Tables I and II we list the parameters  $a_{ij}$ ,  $\sigma_{ij}$  determined by Snider and Herrington. In general the diameters  $\sigma_{ii}$  given here are a little smaller than the effective diameters determined by other means.<sup>(23)</sup> Our results at  $\xi_1^0 = 0.4$  are given in Table III for the various mixtures considered by Snider and Herrington. As is shown,  $\Delta\{\eta\}_a$ ,  $\Delta\{\kappa\}_a$  are appreciable and in many cases predominate over the  $\{\eta\}_E$ ,  $\{\kappa\}_E$ .

Figure 3 shows the trends in  $\Delta\{\eta\}_a$  and  $\Delta\{\kappa\}_a$  ( $\Delta\{\eta\}_a = 0.7794 \Delta\{\kappa\}_a$ ) for mixing of the solute particles of various sizes and strength  $a_{12}$  into the

**Table I. The Snider-Herrington Parameters for a Pure Component**

	Mass (atomic units)	Diameters ( $10^{-8}$ cm)	$a_{11}$ ( $10^{-36}$ cm <sup>3</sup> erg)
Ar	39.94	3.356	4.58
Kr	83.80	3.583	6.79
N <sub>2</sub>	28.02	3.560	4.74
O <sub>2</sub>	32.00	3.338	4.69
CO	28.01	3.597	5.24
CH <sub>4</sub>	16.04	3.701	7.72

**Table II. The Snider-Herrington  $a_{12}$  ( $10^{-36}$  cm<sup>3</sup> erg)**

Ar + K <sub>2</sub>	5.876	Ar + N <sub>2</sub>	4.662
Ar + O <sub>2</sub>	4.852	Ar + CO	4.821
N <sub>2</sub> + O <sub>2</sub>	4.74	N <sub>2</sub> + CO	4.840
CO + CH <sub>4</sub>	6.23	Kr + CH <sub>4</sub>	7.271

**Table III. Intrinsic Shear and Bulk Viscosities of Simple Mixtures at the Solvent (Species 1) Volume Fraction  $\xi_1^0 = 0.4$  and at Temperatures (a) 100 K (b) 150 K (c) 200 K<sup>a</sup>**

Species		$q = \frac{\sigma_{11}}{\sigma_{22}}$	$p = \frac{m_1}{m_2}$	$\{\eta\}_E$	$\Delta\{\eta\}_a$	$\{\kappa\}_E$	$\Delta\{\kappa\}_a$
1	2						
Ar	Kr	0.937	0.477	0.898	(a) 1.179	1.138	1.513
					(b) 0.540		0.693
					(c) 0.350		0.449
Kr	Ar	1.068	2.098	-1.201	(b) -1.202	-1.705	-1.542
					(c) -0.703		-0.902
					(a) -1.061		-1.361
Ar	N <sub>2</sub>	0.943	1.426	-0.314	(c) -0.315	-0.118	-0.404
					(a) 0.942		1.209
					(c) 0.314		0.403
N <sub>2</sub>	Ar	1.061	0.701	0.319	(a) 0.125	-0.283	0.160
					(c) 0.037		0.047
					(a) -0.410		-0.526
O <sub>2</sub>	Ar	0.995	0.801	0.278	(c) -0.117	0.305	-0.150
					(a) -0.948		-1.216
					(c) -0.281		-0.361
CO	Ar	1.072	0.701	0.300	(a) 0.612	0.411	0.785
					(c) 0.194		0.249
					(a) 0.299		-0.239
Ar	CH <sub>4</sub>	0.907	2.490	-0.919	(c) 0.089	-0.239	0.384
					(b) -0.635		1.853
					(c) -0.386		-0.815
CH <sub>4</sub>	Ar	1.103	0.402	0.875	(a) 1.225	0.013	1.572
					(c) 0.408		0.523
					(a) -1.337		-1.715
N <sub>2</sub>	O <sub>2</sub>	1.067	0.876	0.030	(c) -0.381	0.100	-0.489
					(a) 0.160		0.205
					(c) 0.053		0.068
N <sub>2</sub>	CO	0.990	1.000	0.021	(a) -0.336	-0.033	-0.431
					(c) -0.106		-0.136
					(a) 1.062		-0.441
CO	N <sub>2</sub>	1.010	1.000	-0.021	(c) 0.336	-0.441	1.363
					(b) -1.105		0.808
					(c) -0.672		-0.862
CH <sub>4</sub>	CO	1.029	0.573	0.596	(b) -1.036	-0.917	-1.329
					(c) -0.605		-0.776
					(a) 0.160		0.034
Kr	CH <sub>4</sub>	0.968	5.224	-2.026	(c) 0.053	0.034	0.068
					(a) -0.336		-0.431
					(c) -0.106		-0.136
CO	CH <sub>4</sub>	0.972	1.746	-0.655	(a) 1.062	-0.441	1.363
					(c) 0.336		0.431
					(b) -1.105		0.808
CH <sub>4</sub>	CO	1.029	0.573	0.596	(c) -0.672	-0.917	-0.862
					(b) -1.036		-1.329
					(c) -0.605		-0.776
Kr	CH <sub>4</sub>	0.968	5.224	-2.026	(a) 0.160	0.034	0.068
					(c) 0.053		0.068
					(a) -0.336		-0.431
CH <sub>4</sub>	Kr	1.033	0.191	1.528	(b) 0.052	4.201	0.067
					(c) 0.032		4.201
					(a) 0.160		0.034

<sup>a</sup> $\Delta\{\eta\}_a$  and  $\Delta\{\kappa\}_a$  are the contributions from the attractive tails of the interparticle potentials.



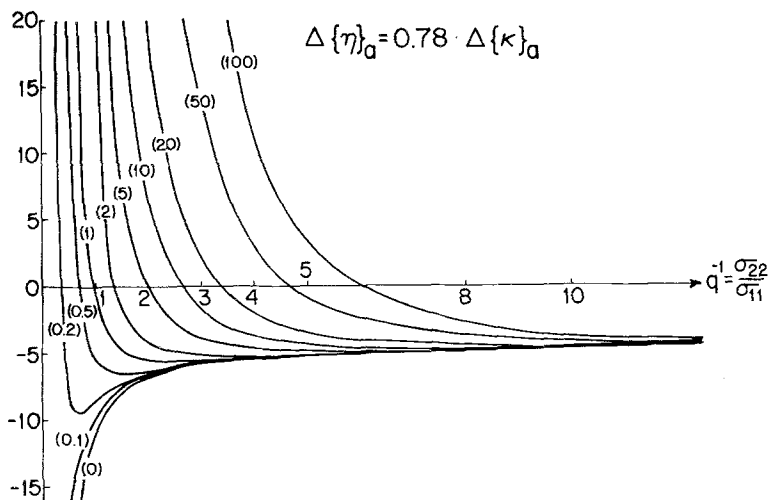


Fig. 3. Contribution of intermolecular attraction to  $\{\eta\}$  and  $\{\kappa\}$  expressed in terms of  $\Delta\{\eta\}_a = 0.78 \Delta\{\kappa\}_a$  for the case  $m_2/m_1 = (\sigma_{22}/\sigma_{11})^3$ ,  $\xi_1^0 = 0.4$ . The numbers in parentheses indicate the ratio  $a_{12}/a_{11}$ .

reference fluid of argon at  $T = 100$  K,  $\xi_1^0 = 0.4$ . For simplicity, we consider the case  $m_2/m_1 = (\sigma_{22}/\sigma_{11})^3$ , i.e., the case in which the mass density of the solute and solvent particles are the same, with the trends plotted for various values of fixed attractive solute-solvent (argon) strength  $a_{12}$ . Figures 4 and 5 represent the general trends of  $\{X\}_E + \Delta\{X\}_a$ . We know of no controllable physical process corresponding to changing the size of the solute particle while holding its attractive solute-solvent interaction strength fixed. Presumably one might be able to experimentally locate a family of solute molecules of different sizes but with roughly the same attractive solute-solvent strength; without such a family with which to compare, Figs. 3, 4, and 5 remain somewhat physically artificial. Nevertheless they are conceptually extremely illuminating. Since the effect of dynamic correlation that Enskog theory neglects is not considered here, the reliability of the results of Figs. 4 and 5 is limited to the case of small solute particles, i.e.,  $\sigma_{22}/\sigma_{11} \lesssim 1$ . However, as far as the  $\Delta\{X\}_a$  themselves are concerned Fig. 3 can be regarded as representing with reasonable accuracy the effect of the attraction, since the inclusion of the infinitely weak, long-range attractive tails does not change the nature of the hard-sphere collision dynamics. As is shown in Figs. 3, 4, and 5, the presence of the attractive tails perturbs the general trends of  $\{X\}$  drastically. If we add only solvent-solvent attraction ( $a_{11} > 0$ ) of strength typical of simple molecules but no solute-solvent attraction [ $a_{12} = 0$  the graphs labeled by (0)] to the pure hard-sphere case

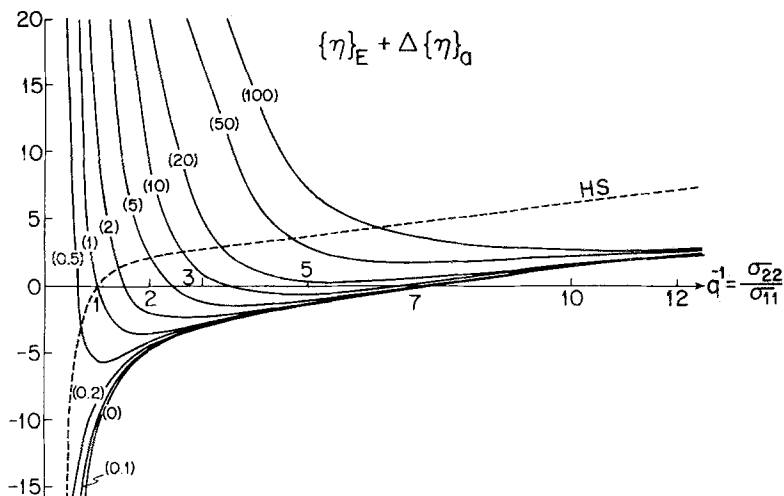


Fig. 4.  $\{\eta\}_E + \Delta\{\eta\}_a$  vs.  $\sigma_{22}/\sigma_{11}$ . Conditions and notations as in Fig. 3. The dashed line represents  $\{\eta\}_E$ .

(shown by the dashed lines), then the intrinsic shear and bulk viscosities are substantially lowered by values that are essentially independent of  $\sigma_{22}/\sigma_{11}$  once this ratio exceeds 3 or so; they respectively approach 4.27 and 5.49 asymptotically as  $\sigma_{22}/\sigma_{11} \rightarrow \infty$ . When we turn on the solute-solvent attraction in addition ( $a_{12} > 0$ ) with  $a_{12}$  comparable to  $a_{11}$ , appreciable change occurs only for  $\sigma_{22}/\sigma_{11}$  less than 3, where the solute-solvent attraction keeps the intrinsic viscosities from becoming extremely negative [as they become when  $\sigma_{22}/\sigma_{11}$  decreases below unity in the absence of the solute-solvent interaction; graphs labeled by (0)]. For  $a_{12}/a_{11} \gtrsim 1$ , in fact,  $\{\eta\}$ ,  $\{\kappa\}$  rapidly increase as  $\sigma_{22}/\sigma_{11}$  decreases past unity, while higher solute-solvent attraction (e.g.,  $a_{12}/a_{11} \gtrsim 15$ ) is enough to keep  $\{\eta\}$ ,  $\{\kappa\}$  positive for all  $\sigma_{22}/\sigma_{11}$ . As the limit  $\sigma_{22}/\sigma_{11} \rightarrow \infty$  is approached with  $a_{12}$  fixed, we observe that the effect of the solute-solvent attraction disappears and thus  $\{X\}$  approaches its value for the case  $a_{12} = 0$ . This is not surprising, since  $a_{12}$  would have to grow along with  $\sigma_{12}$  in order to maintain a nonvanishing effect on the transport as  $\sigma_{22}/\sigma_{11} \rightarrow \infty$ . We note that the method of determining  $M$  via direct measurement of  $\Delta V/V_2$  (2.27) may be the best way of gaining experimental mixing-rule information in finding  $\Delta\{X\}_a$  when the values of  $a_{ij}$  for the mixture under consideration have not already been inferred from other studies.

Since they do not include the effect of dynamic correlation, the Enskog results for  $\{X\}$  can be expected to depart from the true results at

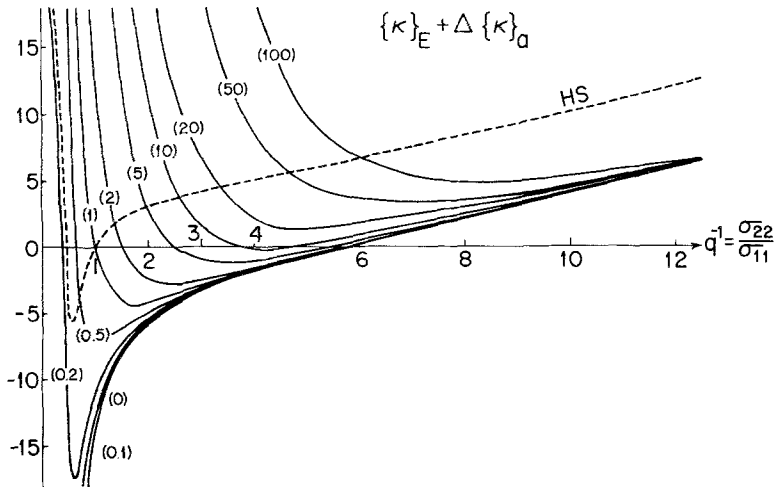


Fig. 5.  $\{\kappa\}_E + \Delta\{\kappa\}_a$  vs.  $\sigma_{22}/\sigma_{11}$ . Conditions and notations as in Fig. 3. The dashed line represents  $\{\kappa\}_E$ .

high values of  $\sigma_{22}/\sigma_{11}$  and at high solvent density. We shall come back to this problem of correcting the Enskog theory in a following paper.

**ACKNOWLEDGMENTS**

G. Stell acknowledges the Office of Basic Energy Sciences, Department of Energy, and W. Sung acknowledges the National Science Foundation, for support of their research. J. Karkheck acknowledges both the above agencies, as well as the Donors of the Petroleum Research Fund, administered by the American Chemical Society, for support of his research. We are indebted to J. R. Dorfman for his helpful comments and suggestions concerning this manuscript.

**APPENDIX**

The Mansoori-Carnahan-Starling-Leland (MCSL) approximation for  $Y_{ij}^{(7)}$  is as follows:

$$\begin{aligned}
 Y_{11} &= (1 - \xi)^{-1} + \frac{3}{2}(1 - \xi)^{-2}(\xi_1 + q\xi_2) + \frac{1}{2}(1 - \xi)^{-3}(\xi_1 + q\xi_2)^2 \\
 Y_{12} &= (1 - \xi)^{-1} + 3(1 + q)^{-1}(1 - \xi)^{-2}(\xi_1 + q\xi_2) + 2(1 + q)^{-2}(\xi_1 + q\xi_2)^2 \\
 Y_{22} &= (1 - \xi)^{-1} + \frac{3}{2}q^{-1}(1 - \xi)^{-2}(\xi_1 + q\xi_2) + \frac{1}{2}q^{-2}(\xi_1 + q\xi_2)^2
 \end{aligned}$$

where

$$\xi = \xi_1 + \xi_2$$

$$\xi_i = \frac{1}{6} \pi n_i \sigma_{ii}^3$$

$$q = \sigma_{11} / \sigma_{22}$$

At  $q = 1$ ,  $Y_{ij}$  is reduced to the Carnahan–Starling  $Y_{11}$  of one-component fluid, which is a nearly exact equation of state. When the last terms of the above expressions are omitted, the  $Y_{ij}$  reduce to the Percus–Yevick  $Y_{ij}$ .

## REFERENCES

1. A. Einstein, *Ann. Phys. (Leipzig)* **19**:289 (1906); **34**:591 (1911).
2. J. Peterson and M. Fixman, *J. Chem. Phys.* **39**:2516 (1963); G. K. Batchelor and J. T. Green, *J. Fluid Mech.* **56**:401 (1972); D. Bedeaux, R. Kapral, and P. Mazur, *Physica* **88A**:88 (1977); G. B. Jeffery, *Proc. R. Soc. (London) Ser. A* **102**:161 (1922).
3. W. A. McElhannon and E. McLaughlin, *Mol. Phys.* **36**:967 (1978).
4. H. van Beijeren and M. H. Ernst, *Physica* **68**:437 (1973); **70**:225 (1973).
5. J. Karkheck and G. Stell, *Phys. Rev. A* **25**: (in press, 1982); *J. Chem. Phys.* **75**:1475 (1981).
6. S. Chapman and T. G. Cowling, *The Mathematical Theory of Nonuniform Gases* (Cambridge University Press, Cambridge, England, 1952).
7. G. A. Mansoori, N. F. Carnahan, K. E. Starling, and T. W. Leland, *J. Chem. Phys.* **54**:1523 (1971).
8. M. K. Tham and K. E. Gubbins, *J. Chem. Phys.* **55**:268 (1971).
9. L. Barajas, L. S. Garcia-Colin, and E. Piña, *J. Stat. Phys.* **7**:161 (1973).
10. P. Resibois, *Phys. Rev. Lett.* **40**:1409 (1978); *Physica* **94A**:1 (1978).
11. J. T. O'Toole and J. S. Dahler, *J. Chem. Phys.* **32**:1097 (1960).
12. H. H. Thorne, see Ref. 6, Chap. 16; J. Karkheck and G. Stell, *J. Chem. Phys.* **71**:3636 (1979).
13. W. Sung and G. Stell, SUSB CEAS report No. 353 (Oct. 1980).
14. H. van Beijeren and J. R. Dorfman, *J. Stat. Phys.* **23**:335 (1980); **24**:445 (1980).
15. B. J. Alder, W. E. Alley, and J. H. Dymond, *J. Chem. Phys.* **61**:1415 (1974).
16. D. Chandler, *Acc. Chem. Res.* **7**:246 (1974); J. H. Dymond and B. J. Alder, *J. Chem. Phys.* **45**:2061 (1966); J. H. Dymond, *Physica A* **75**:100 (1974).
17. J. Piasecki and R. Resibois, *J. Math. Phys.* **14**:1984 (1973); R. Resibois, J. Piasecki, and Y. Pomeau, *Phys. Rev. Lett.* **28**:882 (1972).
18. M. Kac, G. Uhlenbeck, and P. C. Hemmer, *J. Math. Phys.* **4**:216, 229 (1963); **5**:60 (1964); J. L. Lebowitz, G. Stell, and S. Baer, *ibid.* **4**:1382 (1964).
19. N. F. Carnahan and K. E. Starling, *J. Chem. Phys.* **51**:635 (1969).
20. H. C. Longuet-Higgins and B. Widom, *Mol. Phys.* **8**:549 (1964).
21. J. D. van der Waals, *Z. Phys. Chem.* **5**:133 (1890).
22. N. S. Snider and T. M. Herrington, *J. Chem. Phys.* **47**:2248 (1967).
23. L. Verlet, *Phys. Rev.* **159**:98 (1967).